Analysis in Theory and Applications
Anal. Theory Appl., Vol. **42**, No. 1 (2026), pp. 15-31

DOI: 10.4208/ata.2026.deng90.05
March 2026

A Signal Separation Method Based on Instantaneous Frequency Embedded Continuous Wavelet Transform and Short-Time Fourier Transform

Qingtang Jiang*

Department of Mathematics & Statistics, University of Missouri-St. Louis, St. Louis, MO 63121, USA

Received 20 February 2024; Accepted (in revised version) 19 July 2025

Dedicated to the memory of Prof. Donggao Deng on the occasion of his 90th birthday

Abstract. Modeling a non-stationary, multicomponent signal as a superposition of frequency components, each with a well-defined instantaneous frequency (IF), is crucial for extracting information, such as the underlying dynamics hidden within the signal. The synchrosqueezing transform (SST) has emerged as an alternative to empirical mode decomposition (EMD) for separating non-stationary signals. However, because the SST estimates the IFs of all frequency components based on a single phase transformation, its accuracy can be limited. To address this, SST variants based on the IF-embedded short-time Fourier transform (IFE-STFT) and the IF-embedded continuous wavelet transform (IFE-CWT) were developed.

More recently, a direct time-frequency method called the signal separation operation (SSO) was introduced for multicomponent signal separation. SSO bypasses the second step of the two-step SST method for component recovery and is based on variants of the STFT or CWT. In this paper, we propose a direct signal separation method by combining the SSO method with IFE-CWT and IFE-STFT, creating the IFE-CWT-based SSO (IWSSO) and the IFE-STFT-based SSO (IFSSO). Both IWSSO and IFSSO directly separate multicomponent signals without the squeezing operation inherent in SST. Our algorithms and techniques yield more accurate instantaneous frequency estimates and signal separation than conventional SSO or SST methods.

Key Words: Instantaneous frequency (IF) estimation, mode retrieval, signal separation operator based on IF–embedded continuous wavelet transform.

AMS Subject Classifications: 94A12, 42C40, 65160

*Corresponding author. *Email address:* jiangq@umsl.edu (Q. Jiang)

1 Introduction

Recently the synchrosqueezing transform (SST) has been developed to sharpen the time-frequency representation of a non-stationary signal and to recover $x_k(t)$ of a multicomponent signal in the form of (see [1,2] and refer to the references in [3] on the variants of SST)

$$x(t) = A_0(t) + \sum_{k=1}^{K} x_k(t), \quad x_k(t) = A_k(t)\cos\big(2\pi\phi_k(t)\big), \tag{1.1}$$

where $A_k(t) > 0$, $\phi_k'(t) > 0$ with $A_k(t)$ changing slowly.

To recover individual component $x_k(t)$, the SST method consists of two steps. First IF $\phi'_k(t)$ of $x_k(t)$ is estimated from the SST plane. Secondly, after IF was recovered, $x_k(t)$ is computed by a definite integral along each estimated IF curve on the SST plane. The reconstruction accuracy for $x_k(t)$ depends heavily on the accuracy of the IFs estimation carried out in the first step and the sharpness of SST. On the other hand, a direct time-frequency approach, called signal separation operator or signal separation operation (SSO) scheme, was introduced in [4] for multicomponent signal separation. SSO avoids the second step of the two-step SST method in signal separation. The linear chirp-based SSO model was proposed in [5] and theoretically analyzed in [6]. The SSO approaches in [4–6] are based on STFT or its variants. The SSO signal separation method based on the continuous wavelets has been studied in [7]. In addition, the SSO scheme was extended from the 2-dimensional time-frequency (or time-scale) space to the 3-dimensional space of the time-frequency-chirp rate (or the time-csale-chirp rate respectively) using the chirplet transform for the recovery of components with cross-over IFs [8–10].

In this paper, we propose a direct signal separation method by combining SSO with IFE-CWT and IFE-STFT together respectively to form the IFE-CWT-based SSO (IWSSO) and IFE-STFT-based SSO (IFSSO). Both IWSSO and IFSSO separate multicomponent signals directly, without squeezing operation being involved. Our algorithms result in more accurate component recovery than the coventional SSO or SST method.

The rest of the paper is organized as follows. We propose IWSSO and IFSSO in Sections 2 and 3 respectively. Experimental results are provided in Section 4.

2 Signal separation based on instantaneous frequency-embedded CWT

In this section, we first recall the defintion and some properties of the instantaneous frequency-embedded CWT (IFE-CWT). After that we propose a signal separation method by combining IFE-CWT and SSO together.

2.1 Instantaneous frequency-embedded CWT (IFE-CWT)

We say a function $\psi(t) \in L_2(\mathbb{R})$ is a continuous (or an admissible) wavelet provided that

$$0 < C_\psi := \int_{-\infty}^{\infty} |\widehat{\psi}(\xi)|^2 \frac{d\xi}{|\xi|} < \infty \tag{2.1}$$

holds (see e.g., [11, 12]). The condition $C_\psi < \infty$ is called the admissible condition. In this paper the Fourier transform of a function $x(t) \in L_1(\mathbb{R})$ is defined by

$$\widehat{x}(\xi) = \int_{-\infty}^{\infty} x(t) e^{-i2\pi\xi t} dt,$$

which can be extended to functions in $L_2(\mathbb{R})$ or even a generalized function (tempered distribution). The continuous wavelet transform (CWT) of a signal $x(t) \in L_2(\mathbb{R})$ with a continuous wavelet ψ is defined by

$$W_x(a,b) = \langle x, \psi_{a,b} \rangle = \int_{-\infty}^{\infty} x(t) \frac{1}{a} \overline{\psi\Big(\frac{t-b}{a}\Big)} dt,$$

where $\langle \cdot, \cdot \rangle$ is the inner product of $L_2(\mathbb{R})$, and

$$\psi_{a,b}(t) := \frac{1}{a} \psi\Big(\frac{t-b}{a}\Big).$$

The variables a and b are called the scale and time variables respectively. The signal $x(t)$ can be recovered by the inverse continuous wavelet transform (see e.g., [11–13])

$$x(t) = \frac{1}{C_\psi} \int_{-\infty}^{\infty} \int_{-\infty}^{\infty} W_x(a,b) \psi_{a,b}(t) db \frac{da}{|a|}.$$

A function $x(t)$ is called an analytic signal if it satisfies $\widehat{x}(\xi) = 0$ for $\xi < 0$. If the continuous wavelet ψ is analytic, and

$$0 \neq c_\psi := \int_0^{\infty} \overline{\widehat{\psi}(\xi)} \frac{d\xi}{\xi} < \infty, \tag{2.2}$$

then an analytic signal $x(t) \in L_2(\mathbb{R})$, it can be recovered by another inverse wavelet transform which does not involve the time variable b (refer to [1]):

$$x(b) = \frac{1}{c_\psi} \int_0^{\infty} W_x(a,b) \frac{da}{a}.$$

Furthermore, a real signal $x(t) \in L_2(\mathbb{R})$ can be recovered by the following formula (see [1]):

$$x(b) = \mathrm{Re}\Big(\frac{2}{c_\psi} \int_0^{\infty} W_x(a,b) \frac{da}{a}\Big).$$

For $x(t) = A(t)e^{i2\pi\phi(t)}$ with differentiable $A(t), \phi(t)$, its CWT $W_x(a,b)$ is well defined as long as $\psi(t)$ has certain decay as $|t| \to \infty$ to assure $A(t)\psi(t) \in L_1(\mathbb{R})$. In addition, the above two formulas hold for $x(t) = A(t)e^{i2\pi\phi(t)}$ as long as $\psi(t)$ decays fast enough as $|t| \to \infty$.

The (scaled) Morlet's wavelet defined by

$$\widehat{\psi}(\xi) = e^{-2\sigma^2\pi^2(\xi-\mu)^2} - e^{-2\sigma^2\pi^2(\xi^2+\mu^2)}, \tag{2.3}$$

where $\sigma > 0, \mu > 0$, is a commonly used continuous wavelet. The second term in (2.3) is to assure the improper integrals C_ψ and c_ψ converge.

The authors of [14] introduce instantaneous frequency-embedded CWT (IFE-CWT) as defined below.

Definition 2.1 (IFE-CWT)**.** *Suppose $\varphi(t)$ is a differentiable function with $\varphi'(t) > 0$. Then the* **IFE-CWT** *of $x(t) \in L_2(\mathbb{R})$ with a continuous wavelet ψ is defined by*

$$W_x^{\mathrm{I}}(a,b) := \langle x_{\varphi,b,\xi_0}, \psi_{a,b}\rangle = \int_{-\infty}^{\infty} x(t)e^{-i2\pi\left(\varphi(t)-\varphi(b)-\varphi'(b)(t-b)-\xi_0 t\right)}\frac{1}{a}\overline{\psi\Big(\frac{t-b}{a}\Big)}dt, \tag{2.4}$$

where $\xi_0 > 0$ and

$$x_{\varphi,b,\xi_0}(t) := x(t)e^{-i2\pi\left(\varphi(t)-\varphi(b)-\varphi'(b)(t-b)-\xi_0 t\right)}.$$

Observe that if $x(t) = A(t)\exp(i2\pi\phi(t))$ for some $\phi(t)$ with $\phi'(t) > 0$, then $x_{\varphi,b,\xi_0}(t)$ with $\varphi(t) = \phi(t)$ has IF $\phi'(b) + \xi_0$. Also note that in the definition of generalized SST in [15,16], the frequency demodulation of $x(t)$ is $x(t)\exp\big(-i2\pi(\varphi(t) - \xi_0 t)\big)$.

In the above definition, we assume $x(t) \in L_2(\mathbb{R})$. Actually, the definition of IFE-CWT can be extended to slowly growing functions $x(t)$. It was shown in [14] that a function $x(t)$ in $L_2(\mathbb{R})$ can be recovered by

$$x(b) = \frac{1}{c_\psi}\exp(-i2\pi\xi_0 b)\int_{-\infty}^{\infty} W_x^{\mathrm{I}}(a,b)\frac{da}{|a|}, \tag{2.5}$$

where c_ψ is defined by (2.2).

2.2 Signal separation based on IFE-CWT

The component recovery formula with SSO approach does not involve C_ψ or c_ψ; and hence it does not require ψ satisfy the admissible condition (2.1). Thus, for simplicity, in the following we consider continuous wavelets of the form:

$$\psi_\sigma(t) := \overline{\frac{1}{\sigma}g\Big(\frac{t}{\sigma}\Big)}e^{i2\pi\mu t}, \tag{2.6}$$

where $\sigma > 0$, $\mu > 0$, $g \in L_2(\mathbb{R})$, and $\mu > 0$ is fixed. When g is the Gaussian function defined by

$$g(t) = \frac{1}{\sqrt{2\pi}} e^{-\frac{t^2}{2}}, \tag{2.7}$$

then

$$\widehat{\psi}_\sigma(\xi) = e^{-2\sigma^2\pi^2(\xi-\mu)^2}, \tag{2.8}$$

which is Morlet's wavelet in (2.3) without the second term.

For simplicity of our presentation, we consider the complex version of multi-component signals $x(t)$ of (1.1) with the trend $A_0(t)$ being removed, namely,

$$x(t) = \sum_{k=1}^{K} x_k(t) = \sum_{k=1}^{K} A_k(t) e^{i2\pi\phi_k(t)} \tag{2.9}$$

with $A_k(t), \phi_k'(t) > 0$. In addition, we assume that $\phi_{k-1}'(t) < \phi_k'(t)$, $t \in \mathbb{R}$ for $2 \le k \le K$ and

$$\frac{\phi_k'(t) - \phi_{k-1}'(t)}{\phi_k'(t) + \phi_{k-1}'(t)} \ge \Delta, \quad t \in \mathbb{R}, \quad 2 \le k \le K, \tag{2.10}$$

where $0 < \Delta < 1$. The reader is referred to [4] for the methods to remove the trend $A_0(t)$. The condition (2.10) is called the well-separated condition with resolution Δ.

We assume the following conditions hold:

$$A_k(t) \in L_\infty(\mathbb{R}), \qquad A_k(t) > 0, \qquad t \in \mathbb{R}, \tag{2.11a}$$

$$\phi_k(t) \in C^2(\mathbb{R}), \qquad \inf_{t\in\mathbb{R}} \phi_k'(t) > 0, \qquad \sup_{t\in\mathbb{R}} \phi_k'(t) < \infty, \tag{2.11b}$$

$$|A_k(t+\tau) - A_k(t)| \le \varepsilon_1 |\tau| A_k(t), \qquad t \in \mathbb{R}, \qquad 1 \le k \le K, \tag{2.11c}$$

for $\varepsilon_1 > 0$. When ε_1 is small, (2.11) means $A_k(t)$ changes slowly. We also assume ϕ_k satisfy

$$|\phi_k''(t)| \le \varepsilon_2, \quad t \in \mathbb{R}, \quad 1 \le k \le K, \tag{2.12}$$

where $\varepsilon_2 > 0$ is a small number.

If ε_1 and ε_2 are small, then one has (see [7] for details)

$$W_x(a,b) \approx \sum_{k=1}^{K} x_k(b) \widehat{g}\big(\sigma(\mu - a\phi_k'(b))\big). \tag{2.13}$$

Suppose $\widehat{g}$ is compactly supported on $[-\alpha, \alpha]$ or is *essentially supported* in $[-\alpha, \alpha]$, that is

$$|\widehat{g}(\xi)| \le \tau_0 \quad \text{for } |\xi| \ge \alpha,$$

where $\tau_0 > 0$ is a threshold for zero. Then $x_k(b)\widehat{g}\big(\sigma(b)(\mu - a\phi_k'(b))\big)$ (*essentially*) lies within the scale-time zone Z_k defined by

$$Z_k := \Big\{(a,b) : |\mu - a\phi_k'(b)| < \frac{\alpha}{\sigma},\ b \in \mathbb{R}\Big\}.$$

Thus if

$$\sigma \geq \frac{\alpha}{\mu\Delta},$$

then the well-separated condition (2.10) implies that Z_k, $1 \leq k \leq K$ are non-overlapping.

For a fixed b and a positive $\widetilde{\epsilon}_1$ (possibly depending on b), we let $\mathcal{G}_b$ and $\mathcal{G}_{b,k}$ denote the sets defined by

$$\mathcal{G}_b := \{a :\ |W_x(a,b)| > \widetilde{\epsilon}_1\}, \quad \mathcal{G}_{b,k} := \Big\{a \in \mathcal{G}_b :\ |\mu - a\phi_k'(b)| < \frac{\alpha}{\sigma},\ b \in \mathbb{R}\Big\}.$$

Since $Z_k \cap Z_\ell = \emptyset$ for $k \neq \ell$, and $\mathcal{G}_{b,k} = \mathcal{G}_b \cap Z_k$, we know $\mathcal{G}_{b,k}, 1 \leq k \leq K$ are non-overlapping. Denote

$$\breve{a}_k = \breve{a}_k(b) := \arg\max_{a \in \mathcal{G}_{b,k}} |W_x(a,b)|, \quad k = 1, \cdots, K. \tag{2.14}$$

Then we can use $\mu/\breve{a}_k(b)$ to approximate $\phi_k'(b)$:

$$\phi_k'(b) \approx \frac{\mu}{\breve{a}_k(b)}; \tag{2.15}$$

and most importantly, we may reconstruct each component $x_k(b)$ by simply substituting $\breve{a}_k(b)$ to a in $W_x(a,b)$:

$$x_k(b) \approx W_x(\breve{a}_k(b), b). \tag{2.16}$$

To derive (2.13), the approximation

$$x_k(b+at) = A_k(b+at)e^{i2\pi\phi_k(b+at)} \approx A_k(b)e^{i2\pi(\phi_k(b)+\phi_k'(b)at)}$$

has been used. Note that as a function of t, $A_k(b)e^{i2\pi(\phi_k(b)+\phi_k'(b)at)}$ is a sinusoidal function. The above component recovery method with formula (2.16) is called the sinusoidal signal-based model in [7]. The authors of [7] also proposed the linear chirp-based model which is derived from linear chirp local approximation and provided a more precisely component recovery formula. In this case the condition (2.12) is removed. In particular, when g is the Gaussian window function given by (2.7), then the recovery formula is

$$x_k(b) \approx \sqrt{1 - i2\pi\sigma^2\phi_k''(b)\breve{a}_k(b)^2}\ W_x(\breve{a}_k(b), b). \tag{2.17}$$

In practice, $\phi_k''(b)$ is unknown, and it needs to be estimated. See [7] for the details.

Our IFE-CWT-based SSO algorithm is described below.

Algorithm 2.1 (IFE-CWT-based SSO)**.** Given x of the form (2.9), to recover the ℓ-th component $x_\ell(t)$, $1 \le \ell \le K$, we do the following. Set initial $\ell = K$.

Step 1. Calculate $\breve{a}_\ell = \breve{a}_\ell(b)$ in (2.14) with $W_x(a,b)$.

Step 2. Calculate the IFE-CWT $W_x^{\mathrm{I}}(a,b)$ of $x(t)$ with

$$\varphi'(b) = \mu/\breve{a}_\ell(b), \quad \varphi(b) = \int_0^b \mu/\breve{a}_\ell(\tau)d\tau;$$

and then, obtain the ridge of $|W_x^{\mathrm{I}}(a,b)|$ within $\mathcal{G}_{b,\ell}$:

$$\breve{a}_\ell^{\mathrm{I}}(b) := \arg\max_{a\in\mathcal{G}_{b,\ell}} |W_x^{\mathrm{I}}(a,b)|. \tag{2.18}$$

Step 3. Obtain the recovered component for $x_\ell(t)$ by the formula

$$\breve{x}_\ell^{\mathrm{I}}(b) := W_x^{\mathrm{I}}(\breve{a}_\ell^{\mathrm{I}}(b), b). \tag{2.19}$$

Step 4. Update $x(t)$ (get the remainder): $x(t) - \breve{x}_\ell^{\mathrm{I}}(t) \to x(t)$.

Step 5. Repeat Step 1 to Step 4 with the updated $x(t)$ for $\ell = K-1, K-2, \cdots$ and finally $\ell = 1$.

Note that as long as we obtain the ridge $\breve{a}_\ell^{\mathrm{I}}(b)$, we recover the ℓ-th component $x_\ell(b)$ by simply plugging $\breve{a}_\ell^{\mathrm{I}}(b)$ to a in $W_x^{\mathrm{I}}(a,b)$ as shown in (2.19).

After we get $\breve{x}_\ell^{\mathrm{I}}(t)$, $1 \le \ell \le K$ by Algorithm 2.1 of IWSSO, one can use

$$x(t) - \sum_{\ell=1}^{K-1} \breve{x}_\ell^{\mathrm{I}}(t)$$

to run Step 1 to Step 3 in Algorithm 2.1 with $\ell = K$ to get further recovered $x_K(t)$, denote by $\breve{\breve{x}}_K{}^{\mathrm{I}}(t)$. Then we apply the same procedure to

$$x(t) - \breve{\breve{x}}_K{}^{\mathrm{I}}(t) - \sum_{\ell=1}^{K-2} \breve{x}_\ell^{\mathrm{I}}(t)$$

to get $\breve{\breve{x}}_{K-1}{}^{\mathrm{I}}(t)$, and so on to get other components $\breve{\breve{x}}_{K-2}{}^{\mathrm{I}}(t), \cdots, \breve{\breve{x}}_1{}^{\mathrm{I}}(t)$ one by one. We can repeat this procedure. We call this method the **iterative IWSSO** scheme.

The parameter σ in $\psi_\sigma(t)$ defined by (2.6) is also called the window width in the time-domain of wavelet $\psi_\sigma(b)$. The CWT of $x(t)$ with a time-varying parameter considered

in [17] is defined by

$$\begin{aligned}\widetilde{W}_x(a,b) &:= \int_{-\infty}^{\infty} x(t)\frac{1}{a}\overline{\psi_{\sigma(b)}\Big(\frac{t-b}{a}\Big)}dt\\ &= \int_{-\infty}^{\infty} x(b+at)\frac{1}{\sigma(b)}g\Big(\frac{t}{\sigma(b)}\Big)e^{-i2\pi\mu t}dt,\end{aligned}$$

where $\sigma = \sigma(b)$ is a positive function of b. We call $\widetilde{W}_x(a,b)$ the adaptive CWT of $x(t)$ with respect to ψ_σ.

Denote

$$\widetilde{Z}_k := \Big\{(a,b) : |\mu - a\phi_k'(b)| < \frac{\alpha}{\sigma(b)}, b \in \mathbb{R}\Big\}.$$

We assume $\sigma(b)$ satisfies

$$\sigma(b) \geq \frac{\alpha}{\mu}\frac{\phi_k'(b)+\phi_{k-1}'(b)}{\phi_k'(b)-\phi_{k-1}'(b)}, \quad b \in \mathbb{R}, \quad k = 2, \cdots, K.$$

Then the multi-component signal $x(t)$ is well-separated with $\widetilde{W}_x(a,b)$ (that is $\widetilde{Z}_k \cap \widetilde{Z}_\ell = \emptyset, k \neq \ell$).

For a fixed b and a positive $\widetilde{\epsilon}_1$, denote

$$\widetilde{\mathcal{G}}_b := \{a : \ |\widetilde{W}_x(a,b)| > \widetilde{\epsilon}_1\}, \quad \widetilde{\mathcal{G}}_{b,k} := \Big\{a \in \widetilde{\mathcal{G}}_b : \ |\mu - a\phi_k'(b)| < \frac{\alpha}{\sigma(b)}, \ b \in \mathbb{R}\Big\}.$$

Then $\widetilde{Z}_k \cap \widetilde{Z}_\ell = \emptyset$ for $k \neq \ell$, imply $\widetilde{\mathcal{G}}_{b,k}$, $1 \leq k \leq K$ are non-overlapping.

Let

$$\widetilde{a}_k = \widetilde{a}_k(b) := \arg\max_{a \in \widetilde{\mathcal{G}}_{b,k}} |\widetilde{W}_x(a,b)|, \quad k = 1, \cdots, K. \tag{2.20}$$

Then we can use $\mu/\widetilde{a}_k(b)$ to approximate $\phi_k'(b)$:

$$\phi_k'(b) \approx \frac{\mu}{\widetilde{a}_k(b)} \tag{2.21}$$

and

$$x_k(b) \approx \widetilde{W}_x(\widetilde{a}_k(b), b). \tag{2.22}$$

The method to recover components by formula (2.22) is called the adaptive CWT-based SSO method in [7]. Next we introduce the adaptive IFE-CWT-based SSO.

Algorithm 2.2 (Adaptive IFE-CWT-based SSO)**.** Given x of the form (2.9), to recover the ℓ-th component $x_\ell(t)$, $1 \leq \ell \leq K$, we do the following. Set initial $\ell = K$.

Step 1. Calculate $\widetilde{a}_\ell = \widetilde{a}_\ell(b)$ in (2.20).

Step 2. Calculate the adaptive IFE-STFT $\widetilde{W}_x^{\mathrm{I}}(a,b)$ of $x(t)$ with

$$\varphi'(b)=\mu/\widetilde{a}_\ell(b),\quad \varphi(b)=\int_0^b \mu/\widetilde{a}_\ell(\tau)d\tau;$$

and then, pick up the maximum points of $|\widetilde{W}_x^{\mathrm{I}}(a,b)|$ in $\widetilde{\mathcal{G}}_{b,\ell}$:

$$\widetilde{a}_\ell^{\mathrm{I}}(b):=\arg\max_{a\in\widetilde{\mathcal{G}}_{b,\ell}}|\widetilde{W}_x^{\mathrm{I}}(a,b)|. \tag{2.23}$$

Step 3. Obtain the recovered component for $x_\ell(t)$ by the formula

$$\widetilde{x}_\ell^{\mathrm{I}}(b):=\widetilde{W}_x^{\mathrm{I}}(\widetilde{a}_\ell^{\mathrm{I}}(b),b). \tag{2.24}$$

Step 4. Update $x(t)$ (get the remainder): $x(t)-\widetilde{x}_\ell^{\mathrm{I}}(t)\to x(t)$.

Step 5. Repeat Step 1 to Step 4 with the updated $x(t)$ for $\ell=K-1,K-2,\cdots$ and finally $\ell=1$.

3 Signal separation based on instantaneous frequency-embedded STFT

In this section we consider a signal separation algorithm similar to that in the above section, but based on instantaneous frequency-embedded STFT (IFE-STFT). The (modified) short-time Fourier transform (STFT) of $x(t)\in L_2(\mathbb{R})$ with a window function $h(t)\in L_2(\mathbb{R})$ is defined by

$$V_x(t,\eta)=\int_{\mathbb{R}} x(\tau)h(\tau-t)e^{-i2\pi\eta(\tau-t)}d\tau, \tag{3.1}$$

where t and η are the time variable and the frequency variable respectively.

The original signal $x(t)$ can be recovered back from its STFT:

$$x(t)=\frac{1}{\|g\|_2^2}\int_{\mathbb{R}}\int_{\mathbb{R}} V_x(t,\eta)\overline{g(t-\tau)}e^{-i2\pi\eta(\tau-t)}d\tau d\eta.$$

If $h(0)\neq 0$, then one can show that $x(t)$ can also be recovered back from its STFT $V_x(t,\eta)$ with integrals involving only η:

$$x(t)=\frac{1}{h(0)}\int_{\mathbb{R}} V_x(t,\eta)d\eta. \tag{3.2}$$

In addition, if the window function $h(t)\in L_2(\mathbb{R})$ is real, then for a real-valued $x(t)\in L_2(\mathbb{R})$, we have

$$x(t)=\frac{2}{h(0)}\mathrm{Re}\Big(\int_0^\infty V_x(t,\eta)d\eta\Big). \tag{3.3}$$

Here we remark that if the window function $h(t)$ is in the Schwarz class $\mathcal{S}$, then STFT $V_x(t,\eta)$ of a slowly growing $x(t)$ with $h(t)$ is well defined. Furthermore, the above formulas still hold. In this paper we assume $h(0) \neq 0$.

In this section we consider the IFE-STFT which is defined as follows.

Definition 3.1 (IFE-STFT)**.** *Suppose $\varphi(t)$ is a differentiable function with $\varphi'(t) > 0$. The* **IFE-STFT** *of $x(t) \in L_2(\mathbb{R})$ with $\varphi(t)$ and a window function $h(t)$ is defined by*

$$V_x^{\mathrm{I}}(t,\eta) := \int_{\mathbb{R}} x(\tau) e^{-i2\pi(\varphi(\tau)-\varphi(t)-\varphi'(t)(\tau-t)-\eta_0\tau)} h(\tau-t) e^{-i2\pi\eta(\tau-t)} d\tau, \tag{3.4}$$

where η_0 is a positive number.

In the above definition, we assume $x(t) \in L_2(\mathbb{R})$. Actually, the definition of adaptive IFE-STFT can be extended to slowly growing functions $x(t)$. IFE-STFT was first introduced and studied in [18], and it was further studied in [19,20].

The original signal $x(t)$ can be recovered back from its IFE-STFT [20]: Let $x(t)$ be a function in $L_2(\mathbb{R})$. Then

$$x(t) = \frac{\sigma(t) e^{-i2\pi\eta_0 t}}{h(0)} \int_{\mathbb{R}} V_x^{\mathrm{I}}(t,\eta) d\eta. \tag{3.5}$$

In addition, if $g(t)$ is real, then for real $x(t)$, we have

$$x(t) = \frac{2\sigma(t) e^{-i2\pi\eta_0 t}}{h(0)} \mathrm{Re}\Big(\int_{\mathbb{R}} V_x^{\mathrm{I}}(t,\eta) d\eta \Big). \tag{3.6}$$

The STFT-based SSO method does not require the trend $A_0(t)$ in (1.1) be removed, see [6]. In this case, we denote $x_0(t) := A_0(t) e^{i2\pi\phi_0(t)}$ with $\phi_0(t) \equiv 0$. We suppose $\widehat{h}$ is compactly supported in $[-\alpha,\alpha]$ for some $\alpha > 0$ or it is *essentially supported* in $[-\alpha,\alpha]$ in the sense that $\widehat{h}(\xi) \approx 0$ for $\xi \notin [-\alpha,\alpha]$. Suppose the components $x_k(t) = A_k(t) e^{i2\pi\phi_k(t)}$ in (2.9) satisfy

$$\phi_k'(t) - \phi_{k-1}'(t) \geq 2\alpha, \quad t \in \mathbb{R}, \quad k = 1, 2, \cdots, K,$$

then ${\phi'}_k(t)$, $k = 1, \cdots, K$ lie in non-overlapping zones O_k:

$$O_k := \{(t,\eta) : |\eta - \phi_k'(t)| < \alpha, t \in \mathbb{R}\}.$$

Namely, $(t, {\phi'}_k(t)) \in \mathcal{Z}_k$ and $O_k \cap O_\ell = \emptyset, k \neq \ell$. Furthermore, under certain condition on $A_k(t)$, $\mathcal{H}_t := \{\eta : \ |V_x(t,\eta)| > \widetilde{\varepsilon}_1\}$ can be expressed as a disjoint union of exactly $K+1$ non-empty sets $\mathcal{H}_{t,k}, 0 \leq k \leq K$ defined by

$$\mathcal{H}_{t,k} := \{\eta \in \mathcal{G}_t : \ |\eta - \phi_k'(t)| < \alpha\}.$$

Denote

$$\widehat{\eta}_0 := 0, \quad \widehat{\eta}_\ell = \widehat{\eta}_\ell(t) := \arg\max_{\eta\in\mathcal{H}_{t,\ell}} |V_x(t,\eta)|, \quad \ell = 1, \cdots, K. \tag{3.7}$$

Then $\widehat{\eta}_\ell(t)$ gives an approximation to $\phi'_\ell(t)$; and in addition,

$$x_\ell(t) := V_x(t, \widehat{\eta}_\ell(t)) \tag{3.8}$$

gives an approximation to the ℓ-th component $x_\ell(t)$. This is the sinusoidal signal-based SSO method. A linear chirp-based model was proposed in [5] and it was theoretical analyzed in [6]. In particular, when

$$h_\sigma(t) = \frac{1}{\sigma\sqrt{2\pi}} e^{-\frac{t^2}{2\sigma^2}}, \tag{3.9}$$

then the recovery formula of the linear chirp-based model is

$$x_\ell(t) \approx \sqrt{1 - i2\pi\sigma^2\phi''_\ell(t)}\; V_x(t, \widehat{\eta}_\ell(t)). \tag{3.10}$$

Our IFE-STFT-based SSO algorithm is described below.

Algorithm 3.1 (IFE-STFT-based SSO)**.** Given x of the form (2.9), to recover the ℓ-th component $x_\ell(t)$, $1 \le \ell \le K$, we do the following. Set initial $\ell = K$.

Step 1. Calculate $\breve{\eta}_\ell = \breve{\eta}_\ell(t)$ in (3.7) with $V_x(t,\eta)$.

Step 2. Calculate the IFE-STFT $V_x^{\mathrm{I}}(t,\eta)$ of $x(t)$ with

$$\varphi'(t) = \breve{\eta}_\ell(t), \quad \varphi(t) = \int_0^t \breve{\eta}_\ell(\tau)d\tau;$$

and then obtain the ridge of $|V_x^{\mathrm{I}}(t,\eta)|$ within $\mathcal{H}_{t,\ell}$:

$$\breve{\eta}_\ell^{\mathrm{I}}(t) := \arg\max_{\eta\in\mathcal{H}_{t,\ell}} |V_x^{\mathrm{I}}(t,\eta)|. \tag{3.11}$$

Step 3. Obtain the recovered component for $x_\ell(t)$ by the formula

$$\breve{x}_\ell^{\mathrm{I}}(t) := V_x^{\mathrm{I}}(t, \breve{\eta}_\ell^{\mathrm{I}}(t)). \tag{3.12}$$

Step 4. Update $x(t)$ (get the remainder): $x(t) - \breve{x}_\ell^{\mathrm{I}}(t) \to x(t)$.

Step 5. Repeat Step 1 to Step 4 with the updated $x(t)$ for $\ell = K-1, K-2, \cdots$ and finally $\ell = 1$.

The above algorithm can be extended to the adaptive IFE-STFT defined by

$$\widetilde{V}_x^{\mathrm{I}}(t,\eta)=\int_{\mathbb{R}} x(\tau)e^{-i2\pi(\varphi(\tau)-\varphi(t)-\varphi'(t)(\tau-t)-\eta_0\tau)}\frac{1}{\sigma(t)}h\Big(\frac{\tau-t}{\sigma(t)}\Big)e^{-i2\pi\eta(\tau-t)}d\tau, \tag{3.13}$$

where $h(t)$ is a window function, ξ_0 is a positive number, $\sigma(t)$ is a positive function t. When $\sigma(t)\equiv 1$, $\widetilde{V}_x^{\mathrm{I}}(t,\eta)$ is the conventional IFE-STFT. For $\widetilde{V}_x^{\mathrm{I}}(t,\eta)$, the window width of window function $\frac{1}{\sigma(t)}h\big(\frac{\tau}{\sigma(t)}\big)$ is $\sigma(t)$ (up to a constant), which is time-varying.

Suppose $\widehat{h}$ is compactly supported in $[-\alpha,\alpha]$ for some $\alpha>0$ or it is *essentially supported* in $[-\alpha,\alpha]$ in the sense that $\widehat{h}(\xi)\approx 0$ for $\xi\notin[-\alpha,\alpha]$. It was shown in [21] that if $\sigma(t)$ satisfies

$$\sigma(t)\geq\frac{2\alpha}{\phi_k'(t)-\phi_{k-1}'(t)},\quad t\in\mathbb{R},\quad k=1,2,\cdots,K,$$

then $\phi'_k(t)$, $k=1,\cdots,K$ lie in non-overlapping zones $\widetilde{O}_k$:

$$\widetilde{O}_k:=\Big\{(t,\eta):|\eta-\phi_k'(t)|<\frac{\alpha}{\sigma(t)},\ t\in\mathbb{R}\Big\}.$$

Namely, $(t,\phi'_k(t))\in Z_k$ and $\widetilde{O}_k\cap\widetilde{O}_\ell=\emptyset, k\neq\ell$. Furthermore, under certain condition on $A_k(t)$, $\widetilde{\mathcal{H}}_t:=\{\eta:\ |\widetilde{V}_x(t,\eta)|>\widetilde{\epsilon}_1\}$ can be expressed as a disjoint union of exactly $K+1$ non-empty sets $\mathcal{H}_{t,k}$, $0\leq k\leq K$ defined by

$$\widetilde{\mathcal{H}}_{t,k}:=\Big\{\eta\in\widetilde{\mathcal{H}}_t:\ |\eta-\phi_k'(t)|<\frac{\alpha}{\sigma(t)}\Big\}.$$

Denote

$$\widetilde{\eta}_0:=0,\quad \widetilde{\eta}_\ell=\widetilde{\eta}_\ell(t):=\arg\max_{\eta\in\widetilde{\mathcal{H}}_{t,\ell}}|\widetilde{V}_x(t,\eta)|,\quad \ell=1,\cdots,K. \tag{3.14}$$

Then $\widetilde{\eta}_\ell(t)$ gives an approximation to $\phi'_\ell(t)$; and in addition,

$$\widetilde{x}_\ell(t):=\widetilde{V}_x(t,\widetilde{\eta}_\ell(t)) \tag{3.15}$$

gives an approximation to the ℓ-th component $x_\ell(t)$. This is the adaptive SSO method, see [6]. Our adaptive IFE-STFT-based SSO algorithm is described below.

Algorithm 3.2 (Adaptive IFE-STFT-based SSO)**.** Given x of the form (1.1), to recover the ℓ-th component $x_\ell(t)$, $1\leq\ell\leq K$, we do the following five steps. Set initial $\ell=K$.

Step 1. Calculate $\widetilde{\eta}_\ell=\widetilde{\eta}_\ell(t)$ in (3.14).

Step 2. Calculate the adaptive IFE-STFT $\widetilde{V}_x^{\mathrm{I}}(t,\eta)$ of $x(t)$ with $\varphi'(t)=\widetilde{\eta}_\ell(t)$, $\varphi(t)=\int_0^t\widetilde{\eta}_\ell(\tau)d\tau$; and then, pick up the maximum points of $|\widetilde{V}_x^{\mathrm{I}}(t,\eta)|$ in $\widetilde{\mathcal{H}}_{t,\ell}$:

$$\widetilde{\eta}_\ell^{\mathrm{I}}(t):=\arg\max_{\eta\in\widetilde{\mathcal{H}}_{t,\ell}}|\widetilde{V}_x^{\mathrm{I}}(t,\eta)|. \tag{3.16}$$

Step 3. Obtain the recovered component for $x_\ell(t)$ by the formula

$$\widetilde{x}^{\mathrm{I}}_\ell(t) := \widetilde{V}^{\mathrm{I}}_x(t, \widetilde{\eta}^{\mathrm{I}}_\ell(t)). \tag{3.17}$$

Step 4. Update $x(t)$ (get the remainder): $x(t) - \widetilde{x}^{\mathrm{I}}_\ell(t) \to x(t)$.

Step 5. Repeat Step 1 to Step 4 with the updated $x(t)$ for $\ell = K-1, K-2, \cdots$ and finally $\ell = 1$.

4 Experimental results

We present experiments with our proposed methods in this section. Here we provide two examples, one example for the performance of the IFE-CWT-based SSO and the other for the IFE-STFT-based SSO.

We will use continuous wavelet $\psi = \psi_\sigma$ in (2.8) and the window function $h(t) = h_\sigma(t)$ in (3.9) for STFT. ψ_σ and h_σ depend on the parameter σ, and so are the corresponding CWT and STFT. We let $W_x(a,b,\sigma)$ and $V_x(t,\eta,\sigma)$ denote the corresponding CWT and STFT respectively. The choice of σ affects the performance of a CWT-based or STFT-based method for IF estimation and component recovery. To select σ, some papers use the Rényi entropy, which evaluates the concentration of a time-frequency representation such as STFT, CWT, SST, etc. of a signal [22, 23]. As an example, the Rényi entropy for STFT $V_x(t,\eta,\sigma)$ is defined by

$$E_\sigma := \frac{1}{1-\beta}\log_2 \frac{\int_0^\infty \int_{\mathbb{R}} |V_x(t,\eta,\sigma)|^{2\beta}\, dtd\eta}{\big(\int_0^\infty \int_{\mathbb{R}} |V_x(t,\eta,\sigma)|^2\, dtd\eta\big)^\beta},$$

where $\beta > 2$, see [22]. In this paper we set $\beta = 2.5$. If the Rényi entropy is small, then the time-frequency representation is sharp. In Step 1 in Algorithm 2.1, we will choose σ based on E_σ. Suppose $\sigma_0 := \min_{\sigma>0} E_\sigma$. Our experiments show that our method works better if σ is a fraction c_0 of σ_0 with $c_0 \in [\frac{1}{3}, \frac{1}{2}]$. In this paper we set $\sigma = \frac{1}{3}\sigma_0$. Thus for each ℓ, we let $\sigma = \frac{1}{3}\sigma_0$ in Step 1 of Algorithm 2.1, where σ_0 usually changes for different ℓ. We choose σ in the same way for the iterative IWSSO, and for IFSSO (Step 1 in Algorithm 3.1) and iterative IFSSO.

Let $y(t) = y_1(t) + y_2(t)$ be a two-component signal with

$$\begin{aligned} y_1(t) &= e^{-0.1t}\cos\left(2\pi(10t + t^2 + \frac{1}{4}\cos(8t)\right), \\ y_2(t) &= 2e^{0.1\sqrt{t}}\cos\big(2\pi(18t + t^2)\big), \quad t \in [0,4). \end{aligned}$$

We set the (uniform) sample rate for this signal to be $\frac{1}{128}$. The waveform $y(t)$ and IFs are shown in the first row of Fig. 1. We use iterative IWSSO with 3 iterations. The recovered

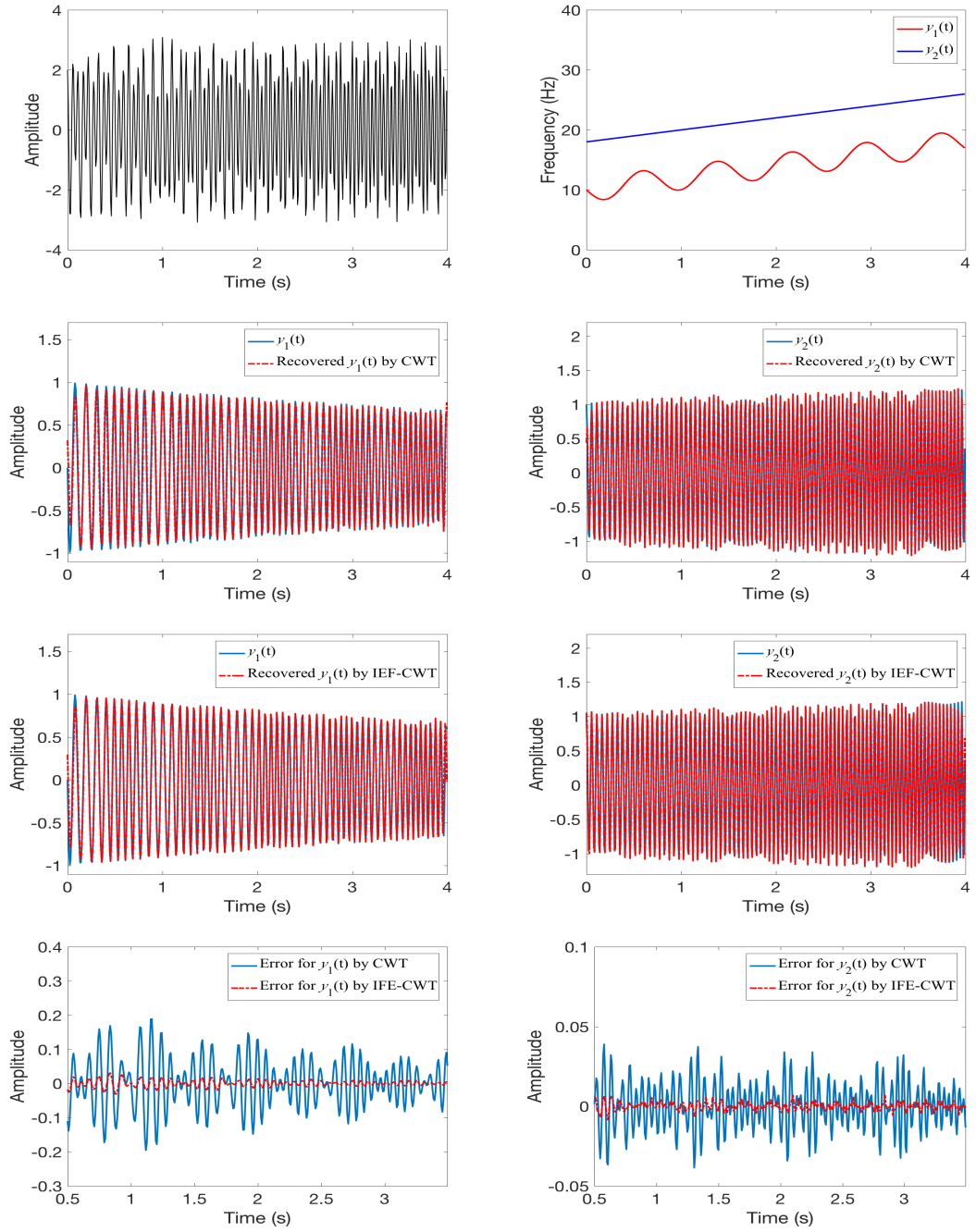

Figure 1: 1st row: waveform (left), IFs ϕ_1' and ϕ_2' (right); 2nd row: recovered $y_1(t)$, $y_2(t)$ by CWT-based SSO; 3rd row: recovered $y_1(t), y_2(t)$ by IFE-CWT-based SSO; 4th row: recovery errors on $[0.5, 3.5)$ for $y_1(t)$ (left panel) and $y_2(t)$ (right panel).

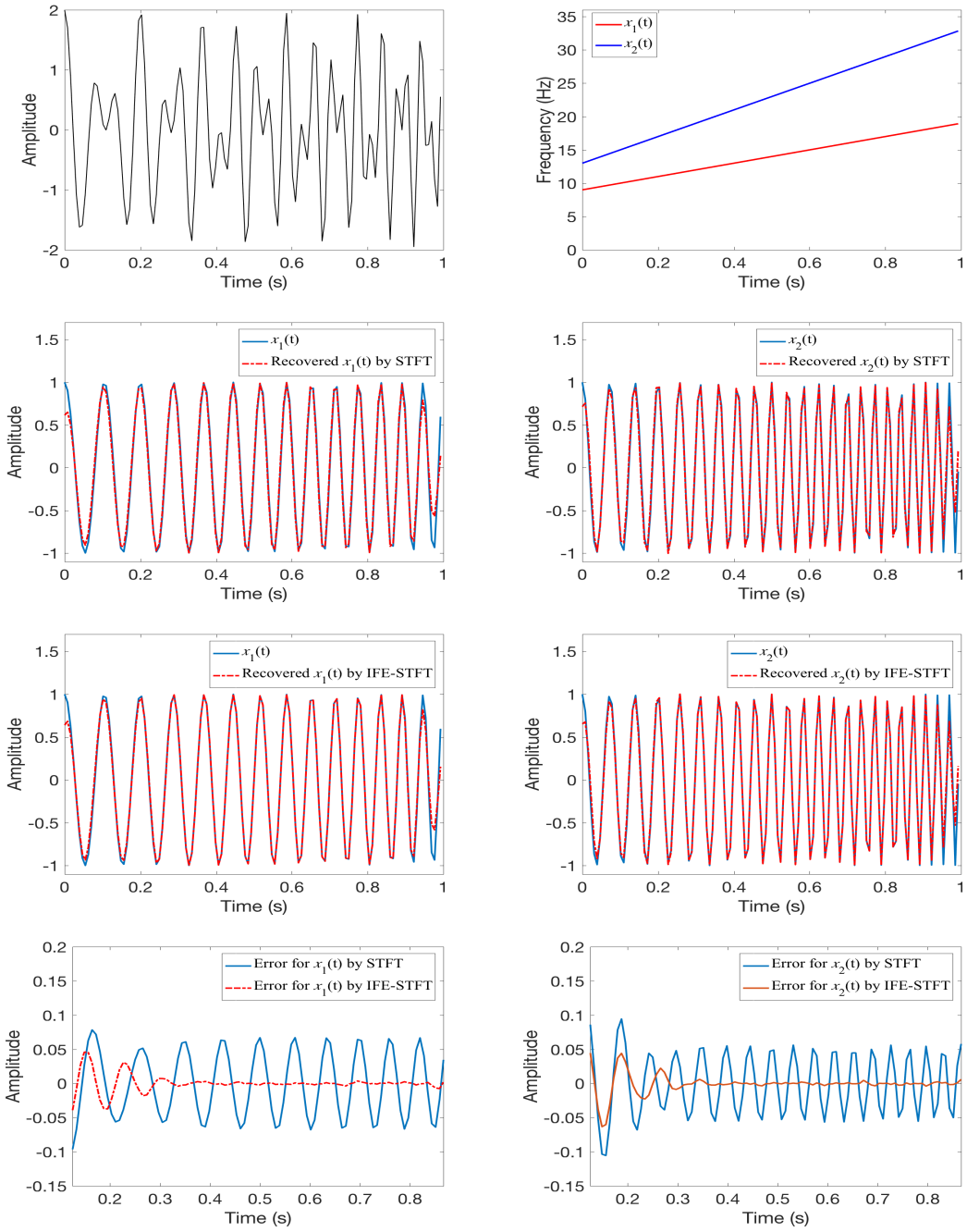

Figure 2: 1st row: waveform (left), IFs ϕ_1' and ϕ_2' (right); 2nd row: recovered $x_1(t)$, $x_2(t)$ by STFT-based SSO; 3rd row: recovered $x_1(t)$, $x_2(t)$ by IFE-STFT-based SSO; 4th row: recovery errors on $[0.125, 0.875)$ for $x_1(t)$ (left panel) and $x_2(t)$ (right panel).

y_1 and y_2 are shown in the 3rd row. For comparison, we apply iterative conventional CWT-based SSO with also 3 iterations to $y(t)$, and the 2nd row shows the component recovery results. Note that the errors near end points 0 and 4 are large. This is caused by the boundary issue. We present the recovery errors on $[0.5, 3.5]$ in the 4th row of Fig. 1. From Fig. 1, we see the proposed IFE-CWT-based SSO performs better than the conventional CWT-based SSO method in signal separation.

Let $x(t) = x_1(t) + x_2(t)$ be another two-component signal with

$$\begin{aligned} x_1(t) &= \cos\left(2\pi(9t + 5t^2)\right), \\ x_2(t) &= \cos\left(2\pi(13t + 10t^2)\right), \quad t \in [0, 1). \end{aligned}$$

$x(t)$ is uniformly sampled with 128 sample points. The waveform $x(t)$ and IFs are shown in the 1st row of Fig. 2. In this example we present the component recovery result for $x(t)$ with iterative IFSSO with 3 iterations. The recovery errors on $[0.125, 0.875)$ are shown in the 2nd row of Fig. 2. As shown in this example, the adaptive IFE-STFT-based method performs much better than the conventional STFT-based SSO method in mode retrieval.

Acknowledgements

The author thanks Drs. Ashley Prater-Bennette and Erin Tripp for their helpful support of this work. This work was approved by AFRL for public release: Distribution unlimited with case number: AFRL-2021-2879.

References

[1] I. Daubechies, J. F. Lu, and H.-T. Wu, Synchrosqueezed wavelet transforms: An empirical mode decomposition-like tool, Appl. Comput. Harmon. Anal., 30(2) (2011), 243–261.
[2] G. Thakur and H.-T. Wu, Synchrosqueezing based recovery of instantaneous frequency from nonuniform samples, SIAM J. Math. Anal., 43(5) (2011), 2078–2095.
[3] Q. T. Jiang, S. X. Li, J. C. Chen, and L. Li, High-order sychrosqueezed time-scale-chirprate transform for mode retrieval of non-stationary signals with crossover instantaneous frequencies, preprint, 2024.
[4] C. K. Chui and H. N. Mhaskar, Signal decomposition and analysis via extraction of frequencies, Appl. Comput. Harmon. Anal., 40(1) (2016), 97–136.
[5] L. Li, C. K. Chui, and Q. T. Jiang, Direct signals separation via extraction of local frequencies with adaptive time-varying parameters, IEEE Trans. Signal Proc., 70 (2022), 2321–2333.
[6] C. K. Chui, Q. T. Jiang, L. Li and J. Lu, Analysis of an adaptive short-time Fourier transform-based multi-component signal separation method derived from linear chirp local approximation, J. Comput. Appl. Math., 396 (2021), 113607.
[7] C. K. Chui, Q. T. Jiang, L. Lin, and J. Lu, Signal separation based on adaptive continuous wavelet-like transform and analysis, Appl. Comput. Harmon. Anal., 53 (2021), 151–179.

[8] L. Li, N. Han, Q. Jiang, and C. K. Chui, A chirplet transform-based mode retrieval method for multicomponent signals with crossover instantaneous frequencies, Digital Signal Proc., 120 (2022), 103262.
[9] C. K. Chui, Q. Jiang, L. Li, and J. Lu, Time-scale-chirprate operator for recovery of non-stationary signal components with crossover instantaneous frequency curves, Appl. Comput. Harmonic Anal., 54 (2021), 323–344.
[10] C. K. Chui, Q. Jiang, L. Li and J. Lu, Analysis of a direct separation method based on adaptive chirplet transform for signals with crossover instantaneous frequencies, Appl. Comput. Harmonic Anal., 62 (2023), 24–40.
[11] Y. Meyer, Wavelets and Operators Volume 1, Cambridge University Press, 1993.
[12] I. Daubechies, Ten Lectures on Wavelets, SIAM, CBMS-NSF Regional Conf. Series in Appl. Math, 1992.
[13] C. K. Chui and Q. T. Jiang, Applied Mathematics–Data Compression, Spectral Methods, Fourier Analysis, Wavelets and Applications, Springer Publ., 2013.
[14] Q. T. Jiang and B. W. Suter, Instantaneous frequency estimation based on synchrosqueezing wavelet transform, Signal Proc., 138 (2017), 167–181.
[15] C. Li and M. Liang, A generalized synchrosqueezing transform for enhancing signal time-frequency representation, Signal Proc., 92(9) (2012), 2264–2274.
[16] S. Meignen, D. H. Pham, and S. McLaughlin, On demodulation, ridge detection, and synchrosqueezing for multicomponent signals, IEEE Trans. Signal Proc., 65(8) (2017), 2093–2103.
[17] L. Li, H. Y. Cai and Q. T. Jiang, Adaptive synchrosqueezing transform with a time-varying parameter for non-stationary signal separation, Appl. Comput. Harmon. Anal., 49 (2020), 1075–1106.
[18] S. B. Wang, X. F. Chen, G. G. Cai, B. Q. Chen, X. Li, and Z. J. He, Matching demodulation transform and synchrosqueezing in time-frequency analysis, IEEE Trans. Signal Proc., 62(1) (2014), 69–84.
[19] S. B. Wang, X. F. Chen, I. W. Selesnick, Y. J. Guo, C. W. Tong and X. W. Zhang, Matching synchrosqueezing transform: A useful tool for characterizing signals with fast varying instantaneous frequency and application to machine fault diagnosis, Mech. Syst. Signal Proc., 100 (2018), 242–288.
[20] Q. T. Jiang, A. Prater-Bennette, B. W. Suter, and A. Zeyani, Instantaneous frequency-embedded synchrosqueezing transform for signal separation, Frontiers in Applied Mathematics and Statistics–Mathematics of Computation and Data Science, 8 (2022), Article 830530.
[21] L. Li, H. Y. Cai, H. X. Han, Q. T. Jiang and H. B. Ji, Adaptive short-time Fourier transform and synchrosqueezing transform for non-stationary signal separation, Signal Proc., 166 (2020), 107231.
[22] L. Stankovic, A measure of some time-frequency distributions concentration, Signal Proc., 81(3) (2001), 621–631.
[23] Y.-L. Sheu, L.-Y. Hsu, P.-T. Chou, and H.-T. Wu, Entropy-based time-varying window width selection for nonlinear-type time-frequency analysis, Int J. Data Sci. Anal., 3 (2017), 231–245.